



## Electrospun nanofibrous composite membranes of chitosan/polyvinyl alcohol-polyacrylonitrile: preparation, characterization, and performance

Farzaneh Hejazi, Seyed Mahmoud Mousavi\*

*Faculty of Engineering, Department of Chemical Engineering, Ferdowsi University of Mashhad, Mashhad, Iran, Tel./Fax: +98 51 38816840; emails: [fa\\_he830@alumni.um.ac.ir](mailto:fa_he830@alumni.um.ac.ir) (F. Hejazi), [mmousavi@um.ac.ir](mailto:mmousavi@um.ac.ir) (S.M. Mousavi)*

Received 11 April 2014; Accepted 24 October 2014

### ABSTRACT

In the present research, double-layer chitosan (CS)/polyvinyl alcohol (PVA) polyacrylonitrile (PAN) and single-layer PAN nanofibrous membranes were prepared by electrospinning method. The blend weight ratio of CS/PVA and concentration of PAN solutions were varied to obtain the optimal electrospun mats in terms of fiber diameter, porosity, and pore size. The 50/50 CS/PVA was determined as the optimal top layer with respect to the obtained results. Moreover, the electrospun nanofibrous membranes were characterized by wastewater treatment. The maximum rejection values of chemical oxygen demand (COD), total dissolved solids (TDS), and turbidity using CS/PVA-PAN nanofibrous composite membranes were 61.14, 34.6, and 99.8%, respectively. Such findings imply that the electrospun nanofibrous composite membranes can be used as appropriate membranes for pretreatment process.

*Keywords:* Electrospun nanofibrous membrane; Polyacrylonitrile; Chitosan; Polyvinyl alcohol; Wastewater treatment

### 1. Introduction

Recently, nanoscale materials have attracted a lot of attention due to their small physical size [1]. Among the other techniques, electrospinning was the simplest and the most effective method for producing ultrafine polymer nanofibers [2]. The standard electrospinning setup comprises three portions: a high-voltage power supply, a spinneret connected to a syringe, and a collector. In this process, a polymer solution is loaded to the syringe and pushed with a syringe pump at a specified rate. As a high voltage is applied, the pendent drop of the polymer solution at the spinneret nozzle will be highly electrified. Then, the electrostatic repulsion force will overcome the sur-

face tension of the polymer solution, which causes stretching of the polymer solution and ejection of a fluid jet. This jet undergoes elongation with a continuous solvent evaporation before deposition on a collector [3] as a nonwoven nanofibrous mat or membrane [4,5].

Electrospun mats showed potential applications in some areas such as filtration, biomedical application, and battery [6,7]. Filtration is the second largest group of nanofiber application. Commercial nanofibrous filters have been used for industrial air cleaning [7]. In liquid filtration, porous polymeric membranes prepared by conventional methods have intrinsic limitations such as low flux and high-fouling performance [8,9]. The characteristics of electrospun nanofibrous membranes such as large surface area-to-volume ratio and highly interconnected pore structure give hope to

\*Corresponding author.

overcome some of these limitations [9]. For instance, Veleirinho and Lopes-da-Silva [9] studied poly(ethylene terephthalate) electrospun nanofibrous membrane filtration for apple juice clarification. They demonstrated that this filtration had high flux performance, less time consumption, and much lower work pressure in comparison with ultrafiltration.

Chitosan (CS) is a natural polysaccharide that has useful properties such as hydrophilicity, biocompatibility, biodegradability, mechanical durability, antimicrobial activity, non-toxicity, and cost-effectiveness [10–12]. The potential applications of nanofibers containing chitin or CS are in many different areas such as filtration, recovery of metal ions, catalyst and enzyme carrier, tissue engineering, drug release, medical implant, wound healing, protective clothing, biosensor, and energy storage [13]. It is necessary to blend CS with other water-soluble polymers like polyvinyl alcohol (PVA) for improvement of CS spinnability [11].

In the present study, CS/PVA electrospun mats with different blend weight ratios were prepared to obtain an optimized nanofibrous mat. As polyacrylonitrile (PAN) is a well-known polymer that possesses good stability and mechanical properties [14], the optimized CS/PVA solution was electrospun on PAN electrospun nanofibrous substrates. The prepared CS/PVA-PAN nanofibrous membranes were cross-linked in glutaraldehyde (GA) solution. In addition, the performance of the electrospun composite membranes in comparison with single-layer PAN membranes was evaluated by filtration of wastewater of food industries.

## 2. Experimental

### 2.1. Materials

PAN ( $M_w = 150,000$ ,  $\rho = 1.184 \text{ g cm}^{-3}$ ) and sodium dodecylbenzene sulfonate (SDBS) were purchased from Aldrich. CS (medium molecular weight and 75–85% deacetylated) and PVA ( $M_w = 72,000$ ,  $\rho = 1.269 \text{ g cm}^{-3}$ ) were obtained from Orbital and Fluka, respectively. *N,N*-dimethylformamide (DMF), acetic acid (glacial), GA (50% solution in water), hydrochloric acid (HCl 37% aqueous solution), and acetone were supplied from Merck. The wastewater was sampled from the food industries effluent obtained from the wastewater treatment plant of a local industrial estate. The values of chemical oxygen demand (COD), total dissolved solids (TDS), and turbidity of the wastewater were in the range of 6,500–7,000  $\text{mg l}^{-1}$ , 500–2,200  $\text{mg l}^{-1}$ , and 900–1,200 NTU, respectively.

### 2.2. Preparation of PAN electrospun nanofibrous mats

PAN was dissolved in DMF for 36–48 h to obtain different homogeneous polymer solutions (9, 11 and 13 wt.%). Then, 0.01 wt.% SDBS was added into the PAN solutions. It was reported that SDBS increased the conductivity, reduced the surface tension, and facilitated the DMF evaporation [15].

The electrospinning apparatus was purchased from Asian Nanostructures Technology Company (ANS-TCO). The solution was held in a syringe with a needle diameter of 0.55 mm. The needle was connected to a power supply. For preparation of the electrospun mats, the fibers were collected on a stainless steel drum having a diameter of 5 cm, covered with aluminum foil. The feed rate and distance between the needle and the collector were  $0.8 \text{ ml h}^{-1}$  and 20 cm, respectively. The rotational and linear speeds of the drum were 300 rpm and  $220 \text{ mm min}^{-1}$ , respectively. The applied voltage was 18 kV.

### 2.3. Preparation of CS/PVA electrospun nanofibrous mats

A specific amount of glacial acetic acid was added into water for preparation of 70 wt.% aqueous acetic acid. PVA solution (8 wt.%) was prepared by dissolving PVA in 70 wt.% aqueous acetic acid under magnetic stirring at  $50^\circ\text{C}$  for 12 h. CS powder was dissolved into 70 wt.% aqueous acetic acid for 12 h to form a 3 wt.% solution. The PVA solution was mixed with the CS solution in CS/PVA weight ratios of 20/80, 30/70, 50/50, 70/30. The feed rate, tip-to-collector distance, and applied voltage were  $0.2 \text{ ml h}^{-1}$ , 10 cm, and 13 kV, respectively. The rotational and linear speeds of the drum were 300 rpm and  $220 \text{ mm min}^{-1}$ , respectively.

### 2.4. Preparation and cross-linking of CS/PVA-PAN nanofibrous membrane

The optimal 50/50 CS/PVA solution was electrospun on the 9 and 11 wt.% PAN substrates. Then, the CS/PVA-PAN membranes were immersed in the GA bath (the concentration of GA was 5% in 95/5 acetone/water solution) for 12 h in order to cross-link hydroxyl groups of PVA. HCl was added as a reaction catalyst to the GA bath. The cross-linked membranes were washed with double-distilled water before use.

### 2.5. Morphological characterization

The morphology of PAN and CS/PVA mats was examined by a scanning electron microscope

(KYKY-EM3200). The mat samples were gold coated by KYKY-SBC12 system before imaging. The average diameter of the electrospun fibers was determined from scanning electron microscopy (SEM) images using Image J software.

### 2.6. Determination of porosity and mean pore size

The samples of prepared mats were cut into specific sizes, and their thickness and mass were measured by a digital micrometer (Insize 3109-25) and an accurate balance (a resolution of 0.1 mg), respectively. The apparent density of the electrospun mats ( $\rho$ ) was calculated by dividing their mass by volume. Thereafter, the porosity of the electrospun mats ( $\varepsilon$ ) was estimated according to the following equation [16,17]:

$$\varepsilon = \frac{(\rho_0 - \rho)}{\rho_0} \times 100\% \quad (1)$$

where  $\rho_0$  is the average density of the polymers used in electrospinning.  $\rho_0$  of the CS/PVA electrospun nanofibrous mats can be calculated by using the following equation [16,17]:

$$\frac{1}{\rho_0} = \frac{\phi_{cs}}{\rho_{cs}} + \frac{\phi_{PVA}}{\rho_{PVA}} \quad (2)$$

where  $\rho_{cs}$  is  $1.342 \text{ g cm}^{-3}$  [18].  $\phi_{cs}$  and  $\phi_{PVA}$  are the mass fraction of CS and PVA, respectively.

The mean pore radius ( $\bar{r}$ ) of the electrospun nanofibrous mats was calculated by using the estimated porosity and mean fiber diameter ( $d$ ) according to the following equation [17,19]:

$$\bar{r} = \frac{\sqrt{\pi}}{4} \left( \frac{\pi}{2 \log\left(\frac{1}{\varepsilon}\right)} - 1 \right) d \quad (3)$$

### 2.7. Permeation and rejection evaluation

Performance tests of the membranes were done by using an experimental setup. For determining pure water flux (PWF), distilled water was passed through the membrane module by applying the transmembrane pressure (TMP) of 0.5 bar. PWF was calculated according to the following equation [17,20]:

$$J = \frac{Q}{A \cdot \Delta t} \quad (4)$$

where  $J$  is the flux ( $\text{l m}^{-2} \text{ h}^{-1}$ ),  $Q$  is the permeate volume (l),  $A$  is the effective membrane area ( $\text{m}^2$ ) and  $\Delta t$  is the sampling time (h).

The treatment performance of nanofibrous membranes was studied using the wastewater at a TMP of 0.5 bar. The permeate flux was calculated by using Eq. (4). The rejection percent of pollution indices of COD, TDS, and turbidity was calculated by using the following equation [20]:

$$R (\%) = \left( 1 - \frac{C_p}{C_f} \right) \times 100 \quad (5)$$

where  $C_p$  and  $C_f$  are the values of each pollution index in the permeate and feed streams, respectively. Turbidity, COD, and TDS were measured by turbidity meter (Lutron TU-2016, Taiwan), COD photometer (CheckitDirect COD, Lovibond, Germany) and conductivity/TDS/Salinity meter (Extech EC400, USA), respectively.

## 3. Results and discussion

### 3.1. The effect of concentration on the morphology of PAN mats

The solution viscosity, controlled by polymer concentration, is one of the most effective parameters on the morphology and fiber size of electrospun mats [21]. Thereby, the 9, 11, and 13 wt.% PAN solutions were used for electrospinning. Fig. 1 shows the SEM image and the fiber diameter distribution of PAN electrospun mats at different concentrations, illustrating that the fabricated fibers are beadless and almost uniform. The 9, 11, and 13 wt.% PAN mats had average fiber diameters of  $332 \pm 21$ ,  $484 \pm 22$ , and  $1,522 \pm 194$  nm, respectively. By increasing the solution concentration while keeping other parameters constant, the average diameter of fibers was increased due to the increase in viscosity and the resistance of the solution against stretching [22].

### 3.2. The effect of the blend weight ratio on morphological structure of CS/PVA mats

The SEM image and fiber diameter distribution of CS/PVA mats at different blend weight ratios under the same processing conditions are shown in Fig. 2. All the fabricated fibers of CS/PVA electrospun mats were beadless and fused at their junction points. It was reported that fusing the fibers of electrospun mats together at their junction points could improve the

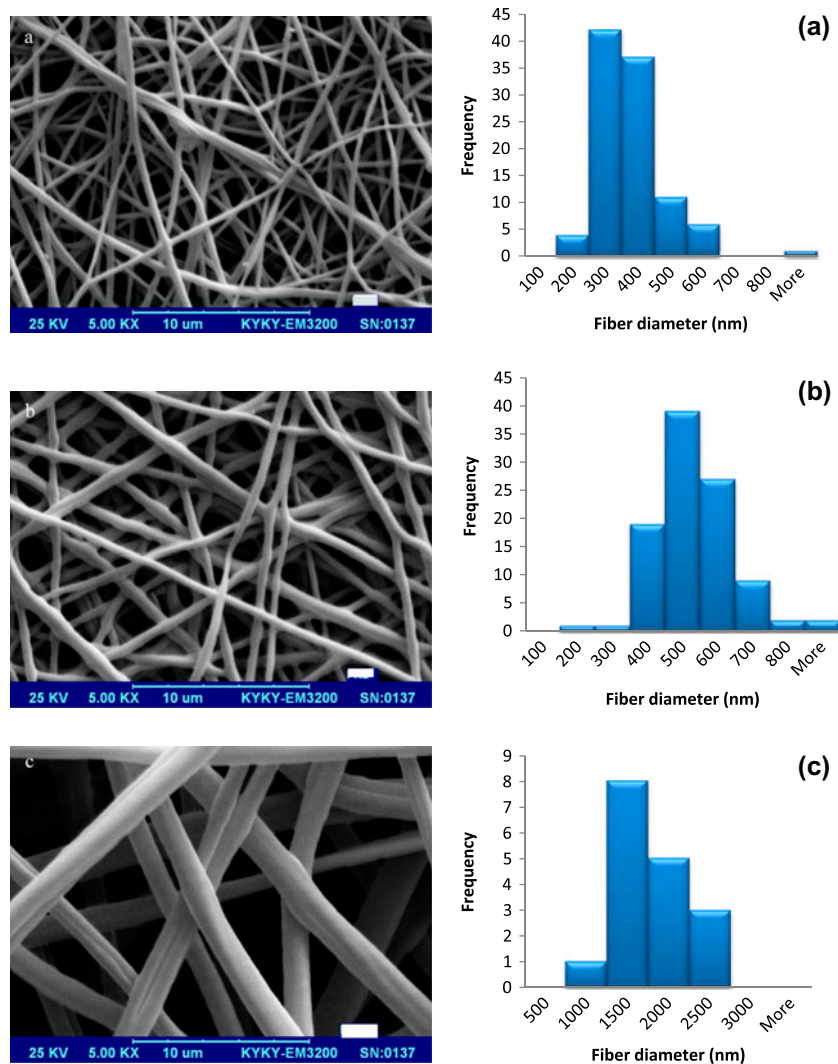


Fig. 1. The SEM image and fiber diameter distribution of (a) 9 wt.%, (b) 11 wt.%, and (c) 13 wt.% PAN electrospun mats.

poor mechanical strength and structural integrity of the mats [23].

The fibers became finer and more uniform with increasing CS content in the blend weight ratio, as the average fiber diameter of 20/80, 30/70, 50/50, and 70/30 CS/PVA electrospun mats was  $351 \pm 16$ ,  $316 \pm 12$ ,  $289 \pm 9$ , and  $264 \pm 9$  nm, respectively. As CS is a linear cationic polymer, it was established that CS can act like other ionic additives [13]. Hence, higher CS content in CS/PVA blend increased the charge density on the jet surface and the jet was more elongated under electrical field [24]. However, with respect to Fig. 2, as the CS content in the blend increased, the fractures of final fibers were increased. Almost the same result was obtained by other researchers [25].

### 3.3. Porosity and mean pore size

The porosity and mean pore size of the electrospun mats are important parameters to evaluate the performance of liquid filtration. Fig. 3 shows the porosity and mean pore size of PAN electrospun mats. The 9, 11, and 13 wt.% PAN mats have the mean pore radius of approximately 2.5, 6, and 19  $\mu\text{m}$ , respectively. When the concentration increased, the mean pore size of PAN electrospun mats became larger because of increasing the porosity of PAN mats from 82 to 87% and the fiber diameter from 332 to 1,522 nm, respectively. It must be noted that real porosities of the mats should be higher than the calculated ones as the thicknesses of the mats were measured under applying pressure of micrometer tip [26].

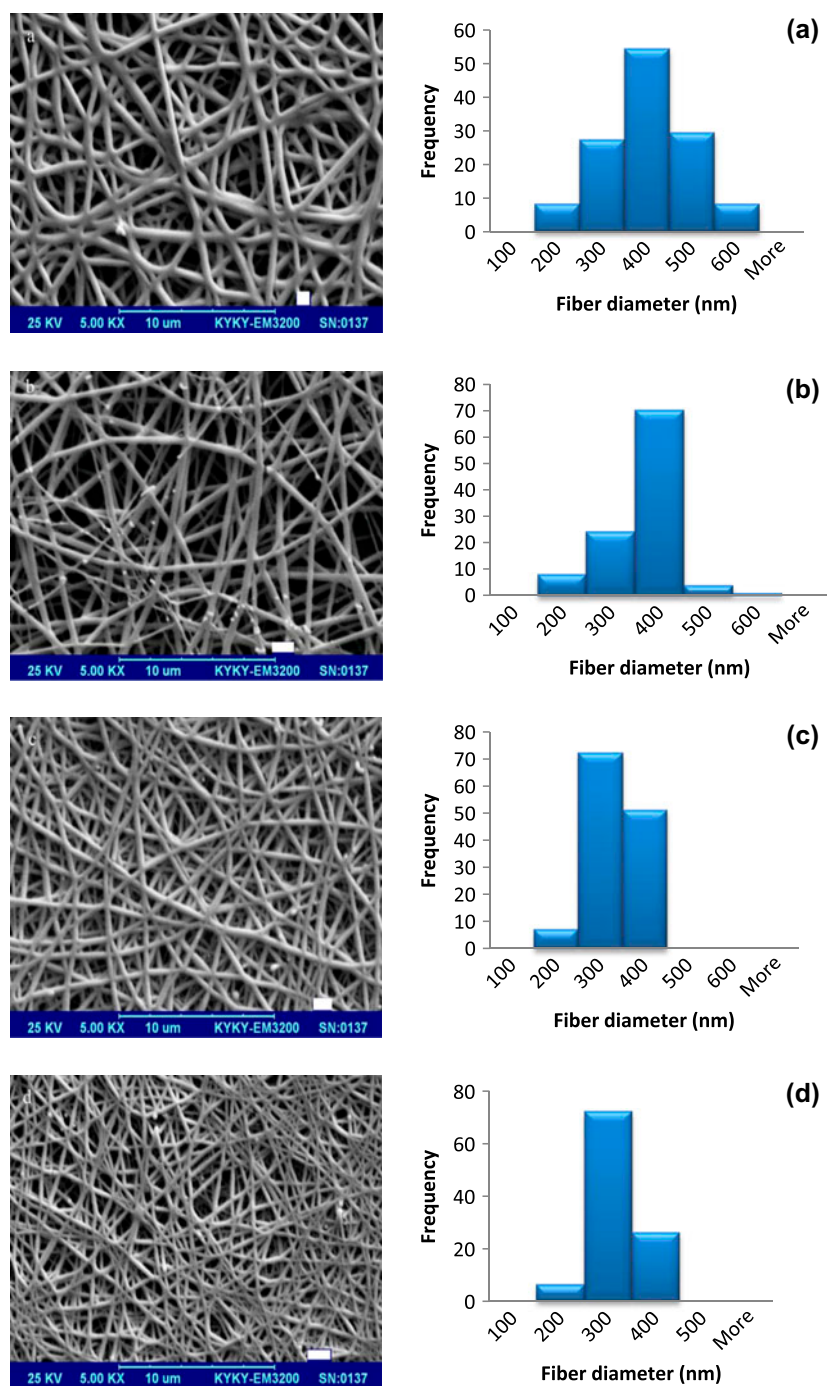


Fig. 2. The SEM image and fiber diameter distribution of (a) 20/80, (b) 30/70, (c) 50/50, and (d) 70/30 CS/PVA electrospun mats.

As mentioned in Section 3.2, by increasing the CS content in the blend, the fiber diameter of the mats became finer, so that the porosity and mean pore size reduced as illustrated in Fig. 4. However, the porosity and mean pore radius of 70/30 CS/PVA electrospun mat increased to 56% and 0.6  $\mu\text{m}$ , respectively. This

behavior is probably due to the toughness recovery in higher CS concentrations [27] that caused an increase in the porosity and mean pore radius.

Because of the broad distribution of fiber diameter and also large fiber diameter and mean pore size of 13 wt.% PAN mat, it was not selected as a separate

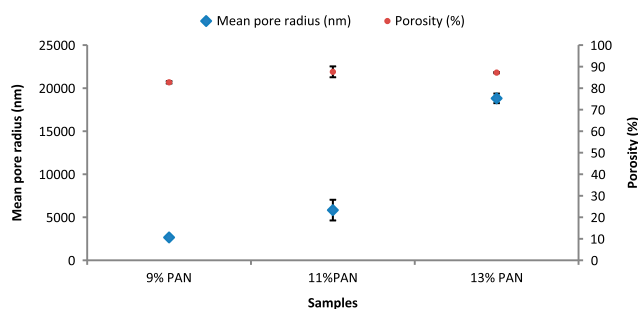


Fig. 3. Porosity and mean pore size of PAN electrospun mats.

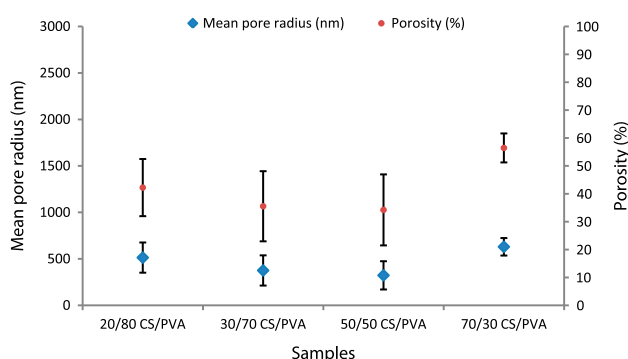


Fig. 4. Porosity and mean pore size of CS/PVA electrospun mats.

membrane and substrate for the composite membrane. Also with respect to the aforementioned results, because of the optimum porosity, mean pore size, fiber diameter, fiber diameter distribution and fiber fracture of 50/50 CS/PVA mat, its solution was selected for electrospinning on the electrospun nanofibrous PAN substrates as presented in Table 1.

#### 3.4. PWF

To discuss about PWF of the prepared electrospun membranes, several parameters such as hydrophilicity, porosity, and pore size should be taken into account. The permeance behavior of the electrospun membranes

Table 1  
Final prepared membranes and their composition

Membrane name	Composition
PAN 1	9 wt.% PAN
PAN 2	11 wt.% PAN
PAN-CS 1	9 wt.% PAN+50/50 CS/PVA
PAN-CS 2	11 wt.% PAN+50/50 CS/PVA

can be expressed by Hagen–Poisseuille's equation (Eq. (6)) [26]:

$$J = \frac{\varepsilon r^2 \Delta p}{8\mu\tau \Delta x} \quad (6)$$

where  $J$  is the water flux ( $\text{m}^3 \text{s}^{-1}$ ),  $\varepsilon$  is the porosity (–),  $r$  is the pore radius (m),  $\tau$  is the tortuosity (–),  $\Delta p$  is the pressure difference across the membrane (Pa),  $\mu$  is the dynamics viscosity (Pa s) and  $\Delta x$  is the membrane thickness (m).

According to this equation, by increasing the pore size and porosity at higher polymer concentrations and considering all the other variables constant, the PWF of PAN 2 is more than that of PAN 1 as seen in Fig. 5.

Addition of 50/50 CS/PVA nanofibrous mat to the substrates causes a relatively slight increase in the permeability of electrospun mats, probably due to the water-permeable property of the top layer. The behavior of PAN-CS 1 and PAN-CS 2 is similar to that of PAN 1 and PAN 2, respectively. The PWF results of PAN-CS 1 and PAN-CS 2 show that the substrates play an important role in water permeance of the composite electrospun membranes.

#### 3.5. Filtration performance of the electrospun membranes

The permeate flux of the electrospun membranes is a crucial factor for filtration. The stable permeate fluxes of the prepared membranes are shown in Fig. 6. As shown in this figure, the trend of variation in the membranes' flux is very similar to that of their PWF. However, the membrane fouling reduced the fluxes in comparison with PWFs, as the fluxes of PAN1 and PAN2 were 200 and 300  $\text{l m}^{-2} \text{h}^{-1}$ , respectively, while their PWFs were 800 and 5,700  $\text{l m}^{-2} \text{h}^{-1}$ , respectively.

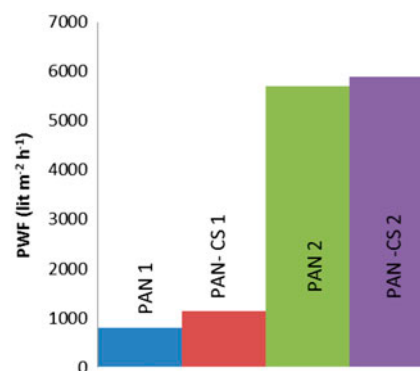


Fig. 5. PWF of the prepared electrospun membranes.

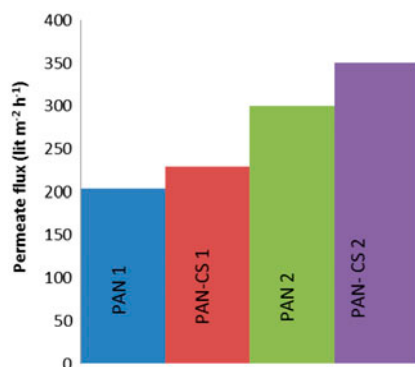


Fig. 6. Permeate flux of the prepared electrospun membranes.

Similar to PWFs, PAN2 flux was more than PAN1 flux due to its larger pore size and porosity. Also, the fluxes of correspondent membranes after addition of CS/PVA on the substrates were decreased in comparison with the PWFs, so that they were 230 and 350 l m<sup>-2</sup> h<sup>-1</sup>, while their PWFs were 1,140 and 6,000 l m<sup>-2</sup> h<sup>-1</sup>, respectively. Furthermore, the fluxes of PAN-CS1 and PAN-CS2 were higher than those of PAN1 and PAN2, respectively. These are probably attributed to the hydrophilicity of the CS/PVA nanofibrous layer.

Electrospun nanofibrous membranes perform as depth filters according to the following explanations. The particles are adsorbed to the nanofibers by three mechanisms of direct interception, inertial impaction, and diffusion (Brownian motion), so that the first group of particles is entrapped within membranes by adsorption and other particles are attached to them afterwards. Thus, the result is a dense cake layer growing from the depth to the surface of electrospun membranes [26]. This behavior causes the prepared electrospun membranes with different porosities and pore sizes to reject almost majority of the wastewater suspended solids even with the size less than their pore size (the turbidity rejection  $\cong$  100%), as it is seen in Table 2, which demonstrates the rejection percent of pollution indices for the electrospun membranes.

Table 2  
Rejection percent of turbidity, COD and TDS for the prepared nanofibrous membranes

Pollution index	PAN 1	PAN 2	PAN-CS 1	PAN-CS 2
Turbidity	99.7	99.5	99.8	99.64
COD	31.38	29.67	61.14	57.88
TDS	30.69	25.66	34.6	27

PAN1 membrane has higher rejection percent than PAN2 membrane because its porosity and pore size are smaller. The COD rejection percent of PAN-CS 1 and PAN-CS 2 in comparison with that of PAN 1 and PAN 2 increased from 31.38 to 61.14% and 29.67 to 57.88%, respectively. Electrospinning the CS/PVA solution on the PAN substrates increases the rejection percent of the wastewater pollution indices, mostly due to lower porosity and pore size of the top layer.

#### 4. Conclusion

The composite membranes containing a CS/PVA top layer and a PAN substrate, as well as single-layer PAN membranes, were prepared by electrospinning and were used for the wastewater treatment.

The CS/PVA electrospun nanofibrous mats were investigated by changing the blend weight ratios. All the CS/PVA electrospun nanofibrous mats were beadless. As the CS content in the blend increased, the fibers became finer but the fractures of fibers increased. Regarding different parameters, the 50/50 blend weight ratio of CS/PVA was chosen as optimum ratio for the top layer of the double-layer membranes. The average fiber diameter, mean pore radius, and porosity of the 50/50 CS/PVA top layer were less than those of the PAN substrates.

The rejection percent of the wastewater pollution indices and fluxes of PAN-CS 1 and PAN-CS 2 were higher than those of PAN1 and PAN2, respectively. Furthermore, the performance tests showed that the prepared electrospun membranes almost rejected the wastewater suspended solids with respect to high rejection of the wastewater turbidity.

#### References

- [1] K. Saeed, S. Haider, T.J. Oh, S.Y. Park, Preparation of amidoxime-modified polyacrylonitrile (PAN-oxime) nanofibers and their applications to metal ions adsorption, *J. Membr. Sci.* 322 (2008) 400–405.
- [2] J. Bai, Q. Yang, M. Li, C. Zhang, L. Yiaoxian, Synthesis of poly(*N*-vinylpyrrolidone)/ $\beta$ -cyclodextrin composite nanofibers using electrospinning techniques, *J. Mater. Process. Technol.* 208 (2008) 251–254.
- [3] J. Liu, J. Shi, E. Secret, L. Wang, H. Zhang, Y. Chen, Parametric optimization of micro-contact printing based thermal transfer of electrospun nanofibers, *Microelectron. Eng.* 87 (2010) 2513–2517.
- [4] C. Tang, C.D. Saquing, J.R. Harding, S.A. Khan, In situ cross-linking of electrospun poly(vinyl alcohol) nanofibers, *Macromolecules* 43 (2010) 630–637.
- [5] K. Ohkawa, D. Cha, H. Kim, A. Nishida, H. Yamamoto, Electrospinning of chitosan, *Macromol. Rapid Commun.* 25 (2004) 1600–1605.

- [6] Z.M. Huang, Y.Z. Zhang, M. Kotaki, S. Ramakrishna, A review on polymer nanofibers by electrospinning and their applications in nanocomposites, *Compos. Sci. Technol.* 63 (2003) 2223–2253.
- [7] A.L. Andrady, *Science and Technology of Polymer Nanofibers*, John Wiley and Sons, Hoboken, NJ, 2008.
- [8] K. Yoon, K. Kim, X. Wang, D. Fang, B.S. Hsiao, B. Chu, High flux ultrafiltration membranes based on electrospun nanofibrous PAN scaffolds and chitosan coating, *Polymer* 47 (2006) 2434–2441.
- [9] B. Veleirinho, J.A. Lopes-da-Silva, Application of electrospun poly(ethylene terephthalate) nanofiber mat to apple juice clarification, *Process Biochem.* 44 (2009) 353–356.
- [10] S. Haider, S.Y. Park, Preparation of the electrospun chitosan nanofibers and their applications to the adsorption of Cu(II) and Pb(II) ions from an aqueous solution, *J. Membr. Sci.* 328 (2009) 90–96.
- [11] H. Liao, R. Qi, M. Shen, X. Cao, R. Guo, Y. Zhang, X. Shi, Improved cellular response on multiwalled carbon nanotube-incorporated electrospun polyvinyl alcohol/chitosan nanofibrous scaffolds, *Colloids Surf. B* 84 (2011) 528–535.
- [12] A. Hussain, G. Collins, D. Yip, C.H. Cho, Functional 3-D cardiac co-culture model using bioactive chitosan nanofiber scaffolds, *Biotechnol. Bioeng.* 110 (2013) 637–647.
- [13] R. Jayakumar, M. Prabakaran, S.V. Nair, H. Tamura, Novel chitin and chitosan nanofibers in biomedical applications, *Biotechnol. Adv.* 28 (2010) 142–150.
- [14] S.K. Nataraj, K.S. Yang, T.M. Aminabhavi, Polyacrylonitrile-based nanofibers—A state-of-the-art review, *Prog. Polym. Sci.* 37 (2012) 487–513.
- [15] D.G. Yu, G.R. Williams, L.D. Gao, S.W. Annie Bligh, J.H. Yang, X. Wang, Coaxial electrospinning with sodium dodecylbenzene sulfonate solution for high quality polyacrylonitrile nanofibers, *Colloids Surf. A*, 396 (2012) 161–168.
- [16] H. Na, Y. Zhao, X. Liu, C. Zhao, X. Yuan, Structure and properties of electrospun poly(vinylidene fluoride)/polycarbonate membranes after hot-press, *J. Appl. Polym. Sci.* 122 (2011) 774–781.
- [17] S.S. Homaeigohar, H. Mahdavi, M. Elbahri, Extraordinarily water permeable sol-gel formed nanocomposite nanofibrous membranes, *J. Colloid Interface Sci.* 366 (2012) 51–56.
- [18] W.C. Hsieh, C.P. Chang, S.M. Lin, Morphology and characterization of 3D micro-porous structured chitosan scaffolds for tissue engineering, *Colloids Surf. B* 57 (2007) 250–255.
- [19] W.W. Sampson, A multiplanar model for the pore radius distribution in isotropic near-planar stochastic fibre networks, *J. Mater. Sci.* 38 (2003) 1617–1622.
- [20] E. Saljoughi, S.M. Mousavi, Preparation and characterization of novel polysulfone nanofiltration membranes for removal of cadmium from contaminated water, *Sep. Purif. Technol.* 90 (2012) 22–30.
- [21] Q.P. Pham, U. Sharma, A.G. Mikos, Electrospinning of polymeric nanofibers for tissue engineering applications: A review, *Tissue Eng.* 12 (2006) 1197–1211.
- [22] S. Ramakrishna, K. Fujihara, W.E. Teo, T.C. Lim, Z. Ma, *An Introduction to Electrospinning and Nanofibers*, World Scientific Publishing CoPte. Ltd., Singapore, 2005.
- [23] B.S. Lalia, E. Guillen-Burrieza, H.A. Arafat, R. Hashaikheh, Fabrication and characterization of poly(vinylidene fluoride-co-hexafluoropropylene (PVDF-HFP) electrospun membranes for direct contact membrane distillation, *J. Membr. Sci.* 428 (2013) 104–115.
- [24] Y.T. Jia, J. Gong, X.H. Gu, H.Y. Kim, J. Dong, X.Y. Shen, Fabrication and characterization of poly (vinyl alcohol)/chitosan blend nanofibers produced by electrospinning method, *Carbohydr. Polym.* 67 (2007) 403–409.
- [25] A. Gholipour K., S.H. Bahrami, M. Nouri, Chitosan-poly(vinyl alcohol) blend nanofibers: Morphology, biological and antimicrobial properties, *e-Polymers* 9 (2009) 1580–1591.
- [26] S.S. Homaeigohar, M. Elbahri, Novel compaction resistant and ductile nanocomposite nanofibrous microfiltration membranes, *J. Colloid Interface Sci.* 372 (2012) 6–15.
- [27] E.S. Costa-Júnior, E.F. Barbosa-Stancioli, A.A.P. Mansur, W.L. Vasconcelos, H.S. Mansur, Preparation and characterization of chitosan/poly(vinyl alcohol) chemically crosslinked blends for biomedical applications, *Carbohydr. Polym.* 76 (2009) 472–481.